# Highly efficient removal of arsenate and arsenite with potassium ferrate: Role of *in situ* formed ferric nanoparticle

**Yanli Kong**
Anhui University of Technology
**Yaqian Ma**
Anhui University of Technology
**Meng Guo**
Anhui University of Technology
**Zhiyan Huang**
Anhui University of Technology
**Jiangya Ma** (Jiangyama0807@163.com)
Anhui University of Technology
**Yong Nie**
Anhui University of Technology
**Lei Ding**
Anhui University of Technology
**Zhonglin Chen**
Harbin Institute of Technology
**Jimin Shen**
Harbin Institute of Technology

**Research Article**

**Keywords:** Potassium ferrate, Arsenic, Hydrolytic ferric iron oxides, Adsorption, Co-precipitation, Contribution

**Posted Date:** June 7th, 2022

**DOI:** https://doi.org/10.21203/rs.3.rs-1714536/v1

# Abstract

It is well known that the capacity of potassium ferrate (Fe(VI)) for the oxidation of pollutants or co-precipitation and adsorption of hazardous species. However, little information has been paid on the adsorption and co-precipitation contribution of the Fe(VI) resultant nanoparticles, the *in-situ* hydrolytic ferric iron oxides. Here, the removal of arsenate (As(V)) and arsenite (As(III)) by Fe(VI) was investigated, which focused on the interaction mechanisms of Fe(VI) with arsenic, especially in the contribution of the co-precipitation and adsorption of its hydrolytic ferric iron oxides. pH and Fe(VI) played significant roles on arsenic removal, over 97.8% and 98.1% of As(V) and As(III) removal were observed when Fe(VI) : As(V) and Fe(VI) : As(III) were 24 : 1 and 16 : 1 at pH 4, respectively. The removal of As(V) and As(III) by *in-situ* and *ex-situ* formed hydrolytic ferric iron oxides was examined respectively. The results revealed that As(III) was oxidized by Fe(VI) to As(V), and then was removed though co-precipitation and adsorption by the hydrolytic ferric iron oxides with the contribution content was about 1 : 3. While for As(V), it could be removed directly by the *in situ* formed particles from Fe(VI) through co-precipitation and adsorption with the contribution content was about 1 : 1.5. By comparison, As(III) and As(V) were mainly removed through adsorption by the 30 min hydrolytic ferric iron oxides during the *ex-situ* process. The hydrolytic ferric iron oxides size was obviously different in the process of *in-situ* and *ex-situ*, possessing abundant and multiple morphological structures ferric oxides, which was conducive for the efficient removal of arsenic. This study would provide a new perspective for understanding the potential of Fe(VI) treatment on arsenic control.


# 1. Introduction

Arsenic contamination is abundant in drinking water ranks and groundwater which threat to the lives of millions of people throughout the globe, especially in United States, India, Bangladesh, China, Canada, Hungary, Japan, Mexico and Argentina, varying from ~50 to > 3000 µg/L, far higher than that of World Health Organization's recommended limit for drinking water (10 µg/L)(Kuo et al. 2017). Sources of arsenic can be either of natural origin such as soils, sediments and natural waters which contain arsenic or as a result of anthropogenic activities such as processing of petroleum refineries, fossil fuel power plants, nonferrous and smelting(Kolarik et al. 2018). Arsenic is always considered as a highly toxic element that increases risk of developing different types of cancer including skin, bladder, liver, lung and causes damage to immune, nervous and respiratory system(Mertens et al. 2016). Thus, optimizing treatment technologies for arsenic removal is currently of great urgency and high priority in many countries.

The dissolved forms of arsenic in water are predominantly the trivalent arsenite (As(III), such as $H_3AsO_3$, $H_2AsO_3^-$, $HAsO_3^{2-}$) and pentavalent arsenate (As(V), such as $H_3AsO_4$, $H_2AsO_4^-$, $HAsO_4^{2-}$) oxyanions(Guan et al. 2009). Various approaches have been explored for arsenic removal, including coagulation/filtration, adsorption, ion exchange, photo-oxidation, and membrane separation, etc(Kolarik et al. 2018, Matsui et al. 2017). Among them, coagulation and adsorption were viewed as affordable, cheap, and effective methods for large flow rates or high As(V) waters. While for As(III), large number of

investigations have reported that As(III) is more mobile and toxic than that of As(V) and has a low affinity to the surface of various adsorbents compared to As(V)(Jain et al. 2009), thus, it is necessary and recommended a pre-treatment of As(III) oxidized to As(V) before coagulation-precipitation or adsorption processes for As(III) effective removal. Within these technologies, multifunctional water treatment agents for arsenic removal have attracted wide attention of many researchers.

Potassium ferrate [$K_2FeO_4$, Fe(VI)] has been proved to be an environmental friendly agent for treating various organic and inorganic contaminants, which should be attributed to its ability of oxidation, flocculation, adsorption, co-precipitation, disinfection, etc(Lee et al. 2014, Talaiekhozani et al. 2017). As a strong oxidant, especially in acidic conditions, Fe(VI) tends to attack electronrich organic moieties, some kind of inorganic metal ions and metal(II)-iminodiacetic acid complexed species(Acosta-Rangel et al. 2020, Yang et al. 2018). Meanwhile, *in-situ* formed ferric nanoparticles generated in the ferrate reduction process, such as $Fe_2O_3$, FeOOH, armouphous ferric, and these hydrolytic ferric iron oxides possessing the properties of highly dispersed, small in size (nanoparticle), and have abundant hydroxylation group, which could interact with oxidation products through the function of chemical bonds and hydrogen bond and adsorb them(Luo et al. 2021a, b, Yang et al. 2018). Recent research demonstrated that the *in-situ* hydrolytic ferric iron oxides of Fe(VI) played an important role for removing high level of metal ions such as arsenic, cadmium(II), cobalt(II), nickel(II), and copper(II), which might be due to its coagulation, adsorption and co-precipitation(Liu et al. 2017, Wang et al. 2022). Lan et al. (2016). noted that As(III) could be oxidized by Fe(VI) and then adsorption by its in-situ hydrolytic ferric iron oxides. Prucek et al. (2013). examined Fe(VI) could *in-situ* formed ferric nanoparticles with γ-$Fe_2O_3$ as the core and γ-FeOOH as the shell during the arsenic removal process, which reacted with As(III) and As(V) and then removed them from the solution in the form of core-shell nanoparticles and was not easy to leach and re-release into the environment. Wang et al. (2020). showed that As(III) removed with Fe(VI) mainly through forming iron arsenate ($FeAsO_4$) precipitation and by the $Fe(OH)_3$ adsorption. Since Fe(VI) could not only oxidize As(III) to As(V), but also remove As(V) by co-precipitation and adsorption of its *in-situ* hydrolytic ferric iron oxides, the contribution content of the co-precipitation and adsorption of its *in-situ* hydrolytic ferric iron oxides aroused our interest. However, the effect of co-precipitation and adsorption of the *in-situ* hydrolytic ferric iron oxides of Fe(VI) on arsenic removal has not been addressed in literature.

Herein, this study focused on the interaction mechanisms of Fe(VI) and arsenic, especially contribution of the co-precipitation and adsorption of the *in-situ* hydrolytic ferric iron oxides to arsenic removal. The removal of aqueous As(III) and As(V) by Fe(VI) through batch experiments were investigated. The objectives of this paper are (1) to determine the efficiency of Fe(VI) and its different time hydrolytic ferric iron oxides on As(III) and As(V) removal under different Fe(VI) dosage, pH and reaction time; (2) to compare the interaction mechanisms of Fe(VI) on As(III) and As(V) removal; (3) to investigate the contribution content of co-precipitation and adsorption of the *in-situ* hydrolytic ferric iron oxides on As(III) and As(V) removal. This study would provide a new insight into the interaction and mechanisms between arsenic and the hydrolytic ferric iron oxides of Fe(VI).

# 2. Materials And Methods

## 2.1 Preparation and characterization of chemicals

All chemicals were reagent-grade and used without any purification. $Na_2HAsO_3$ and $Na_3AsO_4{\cdot}7H_2O$ were purchased from Sigma and were used to prepare the stock solutions of As(III) and As(V), respectively. Hydrochloric acid (HCl), tetramethylammo-nium hydroxide pentahydrate ($(CH_3)_4NOH{\cdot}5H_2O$, TMA), nitric acid ($HNO_3$) and other reagents were purchased from Sinopharm Chemical Reagent Co., Ltd, China. Fe(VI) was prepared in the laboratory according to a wet method(Huang et al. 2021, Liu et al. 2019). Briefly, calcium hypochlorite and potassium carbonate were used to produce potassium hypochlorite, and then Fe(VI) was produced by reacting potassium hypochlorite and iron nitrate under alkaline conditions with a purity higher than 95% by ABTS detection method(Acosta-Rangel et al. 2020). The tap water which has been left in the open air for 24 h to prepare the water samples for the designed experiments, and the characteristics of the water samples were shown in Table S1.

## 2.2 Jar tests

Jar tests were performed open to the air with a jar testing device (ZR4-6, Shenzhen Zhongrun Co., Ltd.). The jar testing procedure was initiated with a rapid mixing at 300 rpm for 5 min, followed by 200 rpm for 2 min and then slow stirring at 40 rpm for 50 min finally there was a 30 min settling. For the investigation the efficiency of Fe(VI) and its hydrolytic ferric iron oxides on arsenic removal, two sets of samples, termed as "*in-situ*" and "*ex-situ*", were prepared. The "*in-situ*" samples originated from simultaneous additions of Fe(VI) and arsenic to the prepared tap water, after Fe(VI) and arsenic were added, the pH of the solutions was adjusted and the rapid mixing was started immediately. While the "*ex-situ*" samples were formed in two steps. First, Fe(VI) was added to the prepared tap water and adjusted the pH of the solution to the setting pH and by subsequent shaking of the samples for 30 min. Then, arsenic stock solution was added to the mixture prepared in the first step. Moreover, in order to compare the arsenic removal efficiency by the hydrolytic ferric iron oxides of Fe(VI), "1 min ferric oxide" samples were prepared, which were similar to the "*ex-situ*" samples procedure with shaking of the samples for 1 min before arsenic stock solution was added. Note that 0.1 mol/L TMA and HCl were employed to adjust the desired pH during reaction. After each test, an appropriate amount of supernatant was taken, filtrated immediately through a 0.45 μm membrane (Shanghai ANPEL, China), and acidified with concentrated $HNO_3$ for determination of arsenic by ICP-AES (PerkinElmer, Optima 2000, UK). All experiments were carried out in triplicates.

## 2.3 Analytical and characterization techniques

The precipitated flocs were collected for particles size distribution using a Particle size analyzer (MalvernZatasizer Nano ZS90, UK). The surface morphology and elemental content distribution of the flocs were observed using a scanning electron microscope (SEM-EDX, JSM-6490LV, JEOL, Japan). The flocs would be collected and processed, such as centrifugation, lyophilized and grinding, and the crystal structures of the flocs were examined by X-ray diffraction (XRD, D8ADVANCE, BRUCKNER, Germany). To

evaluate the coordination of complexes, a fourier transform infrared spectroscope (FTIR, Nicolet6700, Nico-let, USA) was applied to determine the distribution of functional groups on the flocs. Chemical binding energies of arsenic, iron and oxygen in the precipitates were analyzed by X-ray photoelectron spectroscopy (XPS).

## 3. Results And Discussion

# 3.1 Removal characteristics of As(V) and As(Ⅲ) with Fe(VI)

Fig. 1 showed pH and Fe(VI) dosage have great influence on As(V) and As(III) removal by Fe(VI). As shown in Fig. 1(a), at pH 4.0, the optimal As(V) and As(III) removal were observed of 97.5% and 98.3% under 6 mg/L and 4 mg/L Fe(VI), respectively. In addition, the concentrations of As(V) and As(III) in the filtrate were about 6.33 and 4.23 μg/L, lower than that of the limit (10 μg/L) specified by the Chinese drinking water standard (GB5749-2006). Obviously, the removal of As(V) and As(III) increased as Fe(VI) dosage increased. As(V) removal experienced a considerable increased from 15.7% to 90.9% as Fe(VI) dosage increased from 0.5 mg/L to 4.0 mg/L and then slowly increased to the optimum removal rate with increasing Fe(VI) dosage to 6 mg/L(mFe(V)/mAs=24). For the case of As(III) removal, it showed a similar trend to that of As (V) that increased significantly from 14.3% to 98.3% as Fe(VI) dosage increased from 0.5 mg/L to 4.0 mg/L(mFe(V)/mAs=16) and then experienced basically unchanged with further increase Fe(VI) dosage. Note that As(III) removal was slight higher than that of As(V) when Fe(VI) was given a certain amount, which should be mainly associated with promoting the formation of $Fe(OH)_3$ during the oxidation reaction of As(III) to As(V)(Zheng et al. 2021).

As(V) and As(III) removed by Fe(VI) as functions of pH under the corresponding optimal Fe(VI) dosage of 6 mg/L and 4 mg/L respectively were shown in Fig. 1(b). The results showed that As(V) and As(III) removal decreased rapidly from 97.5% to 56.5% and from 98.3% to 51.46% as pH increased from 4.0 to 9.0, respectively. Previous studies have shown that Fe(VI) could oxidize As(III) in one second under acidic conditions, and Fe(VI) would be more easily reduced to iron(III) oxides, the final products of Fe(VI), under this conditions(Yunho et al. 2003). However, Fe(VI) was relatively stable and difficult to be reduced to iron(III) oxides under alkaline conditions, and the corresponding coagulation and adsorption effect was poor(Wang et al. 2022). At the same time, the electrostatic repulsion between the negatively charged iron nanoparticles formed by Fe(VI) and the negatively charged arsenic prevented the interaction between Fe(V) and arsenic under this condition(Wang et al. 2020).

As Fe(VI) was a promising alterative coagulant, the effect of flocculation time on arsenic removal by Fe(VI) was investigated. Fig.S1(a) showed that the residual concentrations of As(V) and As(III) decreased from 250 μg/L to 2.94 and to 0.58 μg/L respectively after 5 min flocculation time under the optimal condition. As the flocculating time increased, the residual content of arsenic decreased slightly, indicating the flocculating time had little effect on arsenic removal. The residual iron content during arsenic removal by Fe(VI) under different pH conditions were shown in Fig.S1(b). The residual iron contents were less than 0.3 mg/L in a wide pH range, which meet the requirements of water quality standards (GB5749-

2006). It indicated that the residual iron content experienced a considerable decrease and then increased trend with pH increased, reached the lowest residual iron content at pH 5.0 with 0.030 mg/L and 0.065 mg/L during As(V) and As(III) removal, respectively. The high residual iron content under alkaline condition might be attributed to the strong stability of Fe(VI) and was difficult to be reduced to iron(III) oxides under this condition.

## 3.2 Removal characteristics of As(V) and As(Ⅲ) with Fe(VI) and ferric oxides

The contribution of Fe(VI) and the hydrolytic ferric iron oxides on As(V) and As(III) removal was examined and demonstrated in Fig. 2. Obviously, the results showed that the oxidation ability of the hydrolytic oxides of Fe(VI) in 1 min were greatly reduced, and the removal of arsenic by the 30min hydrolytic oxides was mainly due to adsorption. As shown in Fig. 2(a), Fe(VI) exhibited remarkable effect on As(V) removal that the residual concentration of As(V) reduced to 2.94 μg/L with the removal rate 98.8%, and the remaining concentration of As(V) was almost unchanged with further the reaction time. While the removal efficiency of As(V) by the 1 min hydrolytic ferric iron oxides decreased. As the reaction time increased from 5 min to 115 min, the residual As(V) concentration was reduced from 16.6 μg/L to 7.40 μg/L with the removal rate increased from 93.4 % to 97.0 %, respectively. As for As(V) removal by the 30 min hydrolytic ferric iron oxides, the removal efficiency was significantly reduced and the residual concentration of As(V) was 83.5 μg/L with the removal rate of 66.6 % at 5 min reaction time, while it reduced to 37.3 μg/L with the removal rate of 85.1 % at 115 min. Therefore, the oxidation of Fe(VI) has little effect on As(V) removal, and the adsorption and co-precipitation of the hydrolytic ferric iron oxides played an important role in the removal of As(V).

As illustrated in Figure 2(b), Fe(VI) showed remarkable effect on As(III) removal, and the residual As(III) concentration decreased to 0.58 μg/L after 5 min, while the removal effect of As(III) by the hydrolytic ferric iron oxides was poor. During As(III) removal by the 1 min hydrolytic ferric iron oxides, the residual As(III) concentration was 151.1 μg/L and the removal rate was only 39.6 % after 5 min reaction time. When the reaction time increased to 115 min, the residual As(III) concentration decreased gradually to 100.2 μg/L with the removal rate 59.9 %. While for As(III) removal by the 30 min hydrolytic ferric iron oxides, the effect of As(III) experienced a considerable decrease. The residual concentration was reduced from 204.8 μg/L to 151.9 μg/L with the removal rate increased from 18.1 % to 39.3 % as reaction time increased from 5 to 115 min, respectively. The above phenomena further illustrated that the mechanisms of As(III) removal by Fe(VI) included the oxidation of Fe(VI), the adsorption and co-precipitation of the hydrolytic ferric iron oxides.

## 3.3 Surface characterization and structure of the characterization

The SEM images of the particles formed in Fe(VI) and the 30 min hydrolytic ferric iron oxides for arsenic removal were investigated to further understand their microscopic morphology, as illustrated in Fig. 3. As shown in Fig. 3a and 3b, the particles produced by Fe(VI) *in-situ* for arsenic removal presented a large number of lamellar structures, of which the particles of As(V) removal were relatively loose and that of As(III) were more dense. Fig. 3c and 3d showed the particles generated in the reaction of arsenic by the 30 min hydrolytic ferric iron oxides that consisted of a large number of spherical particles aggregated. Compared with the *in-situ* removal of arsenic by Fe(VI), the particles formed by the *ex-situ* removal of As(V) from the 30 min hydrolytic ferric iron oxides were more porous and that of As(III) were more dense. The difference of these particles structure between *in-situ* removal of arsenic by Fe(VI) and that of *ex-situ* removal of arsenic by the 30 min hydrolytic ferric iron oxides was related to the different arsenic removal mechanisms. In the process of arsenic removal during *ex-situ* reaction, Fe(VI) self-decomposition formed a spherical hydrolysate, which played an important role in arsenic removal by adsorption and co-precipitation. The elements of the particles formed in Fe(VI) and hydrolytic ferric iron oxides for arsenic removal by EDS analysis were shown in Table S2, as it illustrated, arsenic in solution entered precipitation which indicated arsenic could be effectively removed by Fe(VI) and its hydrolytic ferric iron oxides. In addition, the elements of K, Fe and O in the precipitation should be from Fe(VI).

The size distribution of flocs formed in Fe(VI) and hydrolytic ferric iron oxides for arsenic removal were monitored over the whole flocculation phase. As shown in Fig. S2, the average flocs size validated by three times experiments followed the order: *ex-situ*-As(Ⅲ)＞*ex-situ*-As(V)＞*in-situ*-As(Ⅲ)＞*in-situ* -As(V), with the average size of 59.1 nm, 52.4 nm, 38.0 nm and 35.0 nm, respectively. This result could be consistent with Kralchevska et al. (2016). research on phosphate removal by Fe(VI), which demonstrated that flocs generated in *ex-situ* reaction by hydrolytic iron oxides were smaller and more dense than that of *in-situ* process. In the *ex-situ* process, the particle size would increase with the increase of hydrolysis time, and the harder co-precipitation worked, therefore, floc size was large while arsenic removal efficiency was poor. Moreover, As(V) and As(III) in the process of removing by Fe(VI) would be doped into the hydrolysis oxides earlier and inhibited the growth of the particle size of the hydrolysis oxides.

# 3.4 The composition of flocs

The FTIR spectra of the flocs formed *in-situ* and *ex-situ* of Fe(VI) for arsenic removal was illustrated in Fig. 4A. Specifically, the broadband near 3400 $cm^{-1}$ was assigned to the stretching vibration of hydroxyl groups binding with iron or in $H_2O$ molecules(Ristić et al. 2007). The sharp peak near 1630 $cm^{-1}$ corresponded to the bending vibration of hydroxyl groups in $H_2O$ molecules, indicating the presence of adsorbed water in the samples(Filip et al. 2011). As it shown in Fig. 4A(a), the band at approximately 1450 $cm^{-1}$ and 1375 $cm^{-1}$ attributed to the vibration of $CO_3^{2-}$ and $NO_3^-$, respectively, and $CO_3^{2-}$ might come from water, while $NO_3^-$ should be ascribed to the residues in Fe(VI)(Jia et al. 2007). The peaks at 1400 $cm^{-1}$ and 1053 $cm^{-1}$ observed, indicating that carbonates existed in the flocs of arsenic removal, which should be due to both of the low crystalline and amorphous iron hydroxides were susceptible to $CO_2$ in

the air, as illustrated in Fig. 4A(b-e)(Zhang et al. 2005). The new peaks emerged at 829 $cm^{-1}$ and 833 $cm^{-1}$ should be caused the stretching vibration of As-O-Fe, consistent with the relevant studies which noted that arsenic in the solution co-precipitates with the hydrolysates of Fe(VI)(Jia et al. 2007). In addition, previous studies had showed the main mechanism of As(V) adsorption by amorphous iron oxides was through the formation of inner sphere arsenate complexes on the surface(Cheng et al. 2009, Senn et al. 2018). Moreover, the weak broadband at 829 $cm^{-1}$ also indicated that As(III) removal by hydrolysis products of Fe(VI) was poor. The bank in the region 460-600$cm^{-1}$ was the typical characteristics of low crystallinity rust(Lan et al. 2016), and this conclusion was verified by XRD results that no sharp diffraction peaks observed, indicating the amorphous structure of the arsenic removal flocs (as shown in Figure 4B). The diffraction peaks appeared around the 2 theta value of 26◦, 34◦, 58◦ and 63◦, respectively, which were the spectrum of ferric arsenate and ferric hydroxides according to the JCPDS database(Tang et al. 2011). Lan et al. (2016) also reported that the line 2 hydrous ferric oxides existed in the flocs of As(III) by Fe(VI), which possessed the low crystallinity, high specific surface area and excellent arsenic removal performance.

# 3.5 Binding state of the material elements

The flocs of As(III) and As(V) removal by *in-situ* Fe(VI) and *ex-situ* 30 min hydrolytic ferric iron oxides were collected for XPS analysis to investigate the mechanisms of arsenic removal more accurately, as illustrated in Fig 5, 6, 7 and 8, respectively. The peaks of Fe 2p, O 1s, C 1s, and As 3d were observed in XPS full spectrum (Fig. 5, 6, 7 and 8a), indicating that the obtained residue contained Fe, O, C and As elements. Furthermore, the Fe 2p of the four flocs XPS spectrum results were similar, among them, the peaks near 713 eV, 720 eV and 725 eV correspond to the Fe $2p_{3/2}$, satellite peak and Fe $2p_{1/2}$, indicating that abundant kinds of iron oxides coexisted in the flocs(Kralchevska et al. 2016). For example, iron oxides/hydroxides, such as $Fe_2O_3$□$Fe(OH)_3$ and FeOOH were observed in the four reactive precipitates, as shown in the curve fitting of Fe 2p (Fig.S3) and the same phenomenon has been found in other studies(Liu et al. 2014). Previous studies have shown that Fe(VI) could hydrolysis produces nanoparticles with $Fe_2O_3$ core and FeOOH shell, as $Fe_2O_3$ and FeOOH have similar XPS characteristic peaks(Prucek et al. 2015, Xu et al. 2022), the O1s spectrum of the precipitated product after the reaction was used to investigate the changes of components in details.

The curve fitting of O1s of As(III) removal by *in-situ* Fe(VI) was shown in Fig. 5c, the binding energy peaks at 533.58 eV, 531.38 eV and 529.58 eV were assigned to $H_2O$, $OH^-$ and $O^{2-}$, respectively(Xu et al. 2022). The presence of $H_2O$ indicated the adsorbed water existed in the sample, which was in accordance with the result from the FTIR analysis. The presence of $OH^-$ groups indicated that hydrolytic iron oxides of Fe(VI) existed in the forms as $Fe(OH)_3$ and FeOOH, while that of $O^{2-}$ could be corresponded to FeOOH or $Fe_2O_3$(Liu et al. 2014, Sun et al. 2013). The ratio of the surface $OH^-$ group to $O^{2-}$ could reflect the species of iron oxides and hydroxides in samples. Previous studies have shown that the stoichiometric ratios of

$OH^-$ and $O^{2-}$ in FeOOH were about 0.9-1.1(Liu et al. 2014), which was much less than that of the results in Fig. 5c, confirming that the iron oxide in this sample was mainly $Fe(OH)_3$.

Fig. 5d revealed the forms of arsenic in the flocs that two obvious characteristic peaks near 45 eV and 48 eV were observed, which should belong to the As(V) characteristic peak(Liu et al. 2018), consistent with Prucek et al. (2015) had reported. It is noteworthy the contribution of adsorption and co-precipitation to As(III) removal. In detail, the characteristic peak near 45eV indicated that As(III) was oxidized and then adsorbed on the surface of iron oxide nanoparticles, while that of peak near 48eV might attributed to the oxidized produces As(V) co-precipitated with iron oxide nanoparticles. Therefore, comparing the curve fitting area of adsorbed and co-precipitated, it can be seen that the ratio of the removal amount of As(III) by co-precipitation and adsorption in solution was about 1 : 3.

As illustrated in Fig.6c, the analysis of O1s for removing As(V) flocs by *in-situ* Fe(VI) showed that the binding energy peaks of $H_2O$, $OH^-$ and $O^{2-}$ were located at 534.58 eV, 531.38 eV and 529.38 eV, respectively(Xu et al. 2022). Compared with the removal of As(III) by *in-situ* Fe(VI), the content of adsorbed water was reduced, while the proportion of $OH^-$ and $O^{2-}$ was almost unchanged, indicating that the iron oxide in the sample was mainly $Fe(OH)_3$. As shown in Fig.6d, the results of As 3d analysis showed that the amount of arsenic removed by co-precipitation at 48 eV embedded in nano-oxides and adsorption at 45 eV was about 1 : 1.5. It is noticed that the different contribution content of co-precipitation and adsorption in the As(III) and As(V) removal by *in-situ* Fe(VI) might be due to the somewhat different interaction between arsenic and Fe(VI). That is, the morphology and structure of the two flocs were obviously different, and the intraparticle diffusion of arsenic is favored along the defective, high-energy, and nonequilibrium polycrystalline grain boundary of iron oxides(Tucek et al. 2017).

The O 1s spectra of removing As(III) by *ex-situ* 30 min hydrolytic ferric iron oxides of Fe(VI) was investigated in Fig. 7c, it revealed the binding energy peaks of 535.08 eV, 531.98 eV and 529.78 eV belonged to $H_2O$, $OH^-$ and $O^2$ respectively, among them, the content of $OH^-$ occupied the majority, and that of $H_2O$ and $OH^-$ were relatively low(Xu et al. 2022). Fig. 7d demonstrated the binding energy peaks at 44.58 eV and 45.18 eV corresponded to As $3d_{5/2}$ and As $3d_{3/2}$, where that of As(III) characteristic peak located, implying there was no oxidation existed during As(III) removal under this condition(Wang et al. 2020). It's important to note that the depth of XPS detection is only a few nanometers, reflecting most of the arsenic was present on the outer surface and there was less As(III) embedded in the nano-oxide structure(Yan et al. 2012). Therefore, the results confirmed As(III) removal was mainly through adsorption by the hydrolytic ferric iron oxides of Fe(VI).

Fig.8c showed the O 1s spectra of removing As(V) by *ex-situ* 30 min hydrolytic ferric iron oxides of Fe(VI), the binding energy peaks corresponding to $H_2O$, $OH^-$ and $O^2$ were located at 532.48 eV, 531.28 eV and 529.78 eV, respectively(Xu et al. 2022). The content of $H_2O$ was higher than that of As(III) removal by the hydrolytic ferric iron oxides, while that of $OH^-$ was lower than that of As(III) removal process. The peaks at 45.18eV and 45.78eV belonged to As(V) as shown in Fig.8d, and the depth of probe detected by XPS was

only a few nanometers which implied As(V) removal was enriched mainly by adsorption on the surface of the 30 min hydrolytic ferric iron oxides of Fe(VI)(Yan et al. 2012).

## 3.6 Analysis of the mechanisms on arsenic removal by Fe(VI)

The interpretation of arsenic removal mechanisms and reactivity characteristics were illustrated in Fig. 9 for Fe(VI) and its hydrolytic ferric iron oxides. Under acidic conditions, Fe(VI) has a high reduction potential that can rapidly oxidize As(III) to As(V) in solution. Meanwhile, the *in-situ* iron oxide nanoparticles formed, consisting of low crystalline rust and amorphous iron oxide/hydroxide, such as $Fe_2O_3$, $Fe(OH)_3$, FeOOH, etc, especially $Fe(OH)_3$, and these iron oxides played an important role on arsenic removal. The mechanisms on arsenic removal by Fe(VI) and its *ex-situ* formed hydrolytic ferric iron oxides were clearly different. Arsenic can be removed by adsorption and co-precipitation of the hydrolysis of Fe(VI) in the *in-situ* process. While in the *ex-situ* process, arsenic removal mainly through adsorption by the 30 min hydrolytic ferric iron oxides of Fe(VI). The co-precipitation process consumed the Fe-O-Fe of oxide hydrolyzed by Fe(VI) to generate Fe-O-As, namely, arsenate. While during the adsorption process, arsenic in the solution was adsorbed by the hydrolytic ferric iron oxides and formed an internal spherical complex on the surface. To be specific: in the process of As(III) removed by Fe(VI), As(III) could be oxidized instantaneously and then the formed As(V) removed by co-precipitation and adsorption with iron oxide nanoparticles with the contribution of co-precipitation and adsorption was about 1 : 3. While for As(V) removed by Fe(VI), there was only co-precipitation and adsorption with the iron oxide nanoparticles produced by the *in-situ* hydrolysis of Fe(VI) with the contribution proportion about 1 : 1.5. In addition, adsorption was the mainly mechanism for arsenic removal by ex-situ 30 min hydrolytic ferric iron oxides of Fe(VI), and As(V) removal effect was better than that of As(III) might be due to the low affinity of As(III) to the hydrolytic ferric iron oxides.

## 4. Conclusion

In this study, the effects and mechanisms of As(III) and As(V) removal by Fe(VI) and its hydrolytic ferric iron oxides were investigated. Main conclusions can be drawn as follows:

(1) The dosage of Fe(VI) and pH have significant influence on arsenic removal. When Fe(VI) : As(V) and Fe(VI) : As(III) were 24 : 1 and 16 : 1 at pH 4, the optimum removal efficiency was achieved with the removal rate of 97.8% and 98.1%, respectively. Acidic conditions were conducive for arsenic removal by Fe(VI), while poor arsenic removal efficiency was observed under alkaline conditions, which should be ascribed to the stability of Fe(VI), and the electrostatic repulsion between the generated nanoparticles and arsenic in water under this condition.

(2) The flocs size showed the order of *ex-situ*-As(Ⅲ)＜*ex-situ*-As(V)＜*in-situ*-As(Ⅲ)＜*in-situ* -As(V), with the average size of 59.1 nm, 52.4 nm, 38.0 nm and 35.0 nm, respectively. There are some low crystallinity

ferric arsenate and ferric oxides in the flocs, such as $Fe_2O_3$, $Fe(OH)_3$, FeOOH, etc. especially the $Fe(OH)_3$.

(3) During the process of As(III) removed by Fe(VI), As(III) was oxidized to As(V) and then was removed though co-precipitation and adsorption by the hydrolytic ferric iron oxides with the contribution content was about 1 : 3. While for As(V), it could be removed directly by the *in-situ* formed particles from Fe(VI) through co-precipitation and adsorption with the contribution content of 1 : 1.5. In the *ex-situ* process, the 30 min hydrolytic ferric iron oxides of Fe(VI) do not have the effects of oxidation and with less co-precipitation, thereby, As(III) and As(V) were mainly removed by adsorption by the hydrolytic ferric iron oxides of Fe(VI), furthermore, As (V) removal was higher than that of As(III) mainly ascribed to low affinity of As(III) to the hydrolytic ferric iron oxides under this condition.

# Declarations

Acknowledgments

This study was supported by Natural Science Foundation of Science and Technology Department of Anhui Province (No.2008085QE242), the Open Project of State Key Laboratory of Urban Water Resource and Environment (Harbin Institute of Technology) (No.ES201917), Engineering Research Center of biomembrane water purification and utilization technology (BWPU2020KF08), and National Natural Science Foundation of China (51878001)

### Ethical Approval

Not applicable

### Consent to Participate

**I agree to participate in this called:** Highly efficient removal of arsenate and arsenite with potassium ferrate: Role of in situ formed ferric nanoparticle

Signature of participant: Yanli Kong, Yaqian Ma, Meng Guo, Zhiyan Huang, Jiangya Ma (corresponding author), Yong Nie, Lei Ding, Zhonglin Chen, Jimin Shen.

### Consent to Publish

The author agrees to publication and the copyright to article is transferred to the Journal of Environmental Science and Pollution Research if and when the article is accepted for publication. The author warrants that his/her contribution is original and that he/she has full power to make this grant. The author signs for and accepts responsibility for releasing this material on behalf of any and all co-authors. The copyright transfer covers the exclusive right to reproduce and distribute the article, including reprints, translations, photographic reproductions, microform, electronic form or any other reproductions of similar nature. After submission the agreement signed by the corresponding author, changes of authorship or in the order of the authors listed will not accepted.

### Authors Contributions

Yanli Kong: Conceptualization, Methodology, Investigation, Review & Editing.

Yaqian Ma: Writing, Formal analysis, Data Curation.

Meng Guo: Resources, Investigation, Review & Editing.

Zhiyan Huang: Data Curation, Formal analysis, Visualization.

JiangYa Ma: Resources, Writing - Review & Editing, Supervision, Data Curation.

Yong Nie: Resources, Writing - Review & Editing, Supervision.

Lei Ding: Resources, Writing - Review & Editing.

Zhonglin Chen: Writing: Review & Editing.

Jimin Shen: Writing: Review & Editing.

### Funding

Natural Science Foundation of Science and Technology Department of Anhui Province (No.2008085QE242).

The Open Project of State Key Laboratory of Urban Water Resource and Environment (Harbin Institute of Technology) (No.ES201917).

Engineering Research Center of biomembrane water purification and utilization technology (BWPU2020KF08).

National Natural Science Foundation of China (51878001)

### Competing Interests

The authors declare that they have no known competing financial interests or personal relationships that could have appeared to influence the work reported in this paper.

### Availability of data and materials

The datasets used or analysed during the current study are available from the corresponding author on reasonable request.

## References

Acosta-Rangel A, Sanchez-Polo M, Rozalen M, Rivera-Utrilla J, Polo A, Berber-Mendoza MS, Lopez-Ramon MV (2020): Oxidation of sulfonamides by ferrate(VI): Reaction kinetics, transformation byproducts and toxicity assesment. J ENVIRON MANAGE 255

Cheng HF, Hu YN, Luo J, Xu B, Zhao JF (2009): Geochemical processes controlling fate and transport of arsenic in acid mine drainage (AMD) and natural systems. J HAZARD MATER 165, 13-26

Filip J, Yngard RA, Siskova K, Marusak Z, Ettler V, Sajdl P, Sharma VK, Zboril R (2011): Mechanisms and Efficiency of the Simultaneous Removal of Metals and Cyanides by Using Ferrate(VI): Crucial Roles of Nanocrystalline Iron(III) Oxyhydroxides and Metal Carbonates. CHEM-EUR J 17, 10097-10105

Guan XH, Ma J, Dong HR, Jiang L (2009): Removal of arsenic from water: Effect of calcium ions on As(III) removal in the $KMnO_4$-Fe(II) process. WATER RES 43, 5119-5128

Huang Z, Wang L, Liu Y, Zhang H, Zhao X, Bai Y, Ma J (2021): Ferrate self-decomposition in water is also a self-activation process: Role of Fe(V) species and enhancement with Fe(III) in methyl phenyl sulfoxide oxidation by excess ferrate. WATER RES 197, 117094

Jain A, Sharma VK, Mbuya OS (2009): Removal of arsenite by Fe(VI), Fe(VI)/Fe(III), and Fe(VI)/Al(III) salts: Effect of pH and anions. J HAZARD MATER 169, 339-344

Jia Y, Xu L, Wang X, Demopoulos GP (2007): Infrared spectroscopic and X-ray diffraction characterization of the nature of adsorbed arsenate on ferrihydrite. GEOCHIM COSMOCHIM AC 71, 1643-1654

Kolarik J, Prucek R, Tucek J, Filip J, Sharma VK, Zboril R (2018): Impact of inorganic ions and natural organic matter on arsenates removal by ferrate(VI): Understanding a complex effect of phosphates ions. WATER RES 141, 357-365

Kralchevska RP, Prucek R, Kolarik J, Tucek J, Machala L, Filip J, Sharma VK, Zboril R (2016): Remarkable efficiency of phosphate removal: Ferrate(VI)-induced in situ sorption on core-shell nanoparticles. WATER RES 103, 83-91

Kuo CC, Moon KA, Wang SL, Silbergeld E, Navas-Acien A (2017): The Association of Arsenic Metabolism with Cancer, Cardiovascular Disease, and Diabetes: A Systematic Review of the Epidemiological Evidence. ENVIRON HEALTH PERSP 125

Lan BY, Wang YX, Wang X, Zhou XT, Kang Y, Li LS (2016): Aqueous arsenic (As) and antimony (Sb) removal by potassium ferrate. CHEM ENG J 292, 389-397

Lee Y, Kissner R, von Gunten U (2014): Reaction of Ferrate(VI) with ABTS and Self-Decay of Ferrate(VI): Kinetics and Mechanisms. ENVIRON SCI TECHNOL 48, 5154-5162

Liu A, Liu J, Pan B, Zhang WX (2014): Formation of lepidocrocite (γ-FeOOH) from oxidation of nanoscale zero-valent iron (nZVI) in oxygenated water. RSC ADV 4, 57377-57382

Liu AR, Wang W, Liu J, Fu RB, Zhang WX (2018): Nanoencapsulation of arsenate with nanoscale zero-valent iron (nZVI): A 3D perspective. SCI BULL 63, 1641-1648

Liu YL, Wang L, Wang XS, Huang ZS, Xu CB, Yang T, Zhao XD, Qi JY, Ma J (2017): Highly efficient removal of trace thallium from contaminated source waters with ferrate: Role of in situ formed ferric nanoparticle. WATER RES 124, 149-157

Liu YL, Zhang J, Huang HM, Huang ZS, Xu CB, Guo GJ, He HY, Ma J (2019): Treatment of trace thallium in contaminated source waters by ferrate pre-oxidation and poly aluminium chloride coagulation. SEP PURIF TECHNOL 227

Luo M, Zhou H, Zhou P, Lai L, Liu W, Ao Z, Yao G, Zhang H, Lai B (2021a): Insights into the role of in-situ and ex-situ hydrogen peroxide for enhanced ferrate(VI) towards oxidation of organic contaminants. WATER RES 203, 117548

Luo M, Zhou H, Zhou P, Lai L, Liu W, Ao Z, Yao G, Zhang H, Lai B (2021b): Insights into the role of in-situ and ex-situ hydrogen peroxide for enhanced ferrate(VI) towards oxidation of organic contaminants. WATER RES 203, 117548

Matsui Y, Shirasaki N, Yamaguchi T, Kondo K, Machida K, Fukuura T, Matsushita T (2017): Characteristics and components of poly-aluminum chloride coagulants that enhance arsenate removal by coagulation: Detailed analysis of aluminum species. WATER RES 118, 177-186

Mertens J, Rose J, Wehrli B, Furrer G (2016): Arsenate uptake by Al nanoclusters and other Al-based sorbents during water treatment. WATER RES 88, 844-851

Prucek R, Tucek J, Kolarik J, Filip J, Marusak Z, Sharma VK, Zboril R (2013): Ferrate(VI)-Induced Arsenite and Arsenate Removal by In Situ Structural Incorporation into Magnetic Iron(III) Oxide Nanoparticles. ENVIRON SCI TECHNOL 47, 3283-3292

Prucek R, Tucek J, Kolarik J, Huskova I, Filip J, Varma RS, Sharma VK, Zboril R (2015): Ferrate(VI)-Prompted Removal of Metals in Aqueous Media: Mechanistic Delineation of Enhanced Efficiency via Metal Entrenchment in Magnetic Oxides. ENVIRON SCI TECHNOL 49, 2319-2327

Ristić, Grave M, Eddy, Musić, Svetozar, Popović, Orehovec S, Zvonko (2007): Transformation of low crystalline ferrihydrite to alpha-$Fe_2O_3$ in the solid state. J MOL STRUCT 834-836, 454-460

Senn AC, Hug SJ, Kaegi R, Hering JG, Voegelin A (2018): Arsenate co-precipitation with Fe(II) oxidation products and retention or release during precipitate aging. WATER RES 131, 334-345

Sun YK, Xiong XM, Zhou GM, Li CY, Guan XH (2013): Removal of arsenate from water by coagulation with in situ formed versus pre-formed Fe(III). SEP PURIF TECHNOL 115, 198-204

Talaiekhozani A, Talaei MR, Rezania S (2017): An overview on production and application of ferrate (VI) for chemical oxidation, coagulation and disinfection of water and wastewater. Journal of Environmental Chemical Engineering 5, 1828-1842

Tang WS, Li Q, Gao SA, Shang JK (2011): Arsenic (III,V) removal from aqueous solution by ultrafine alpha-$Fe_2O_3$ nanoparticles synthesized from solvent thermal method. J HAZARD MATER 192, 131-138

Tucek J, Prucek R, Kolarik J, Zoppellaro G, Petr M, Filip J, Sharma VK, Zboril R (2017): Zero-Valent Iron Nanoparticles Reduce Arsenites and Arsenates to As(0) Firmly Embedded in Core-Shell Superstructure: Challenging Strategy of Arsenic Treatment under Anoxic Conditions. ACS SUSTAIN CHEM ENG 5, 3027-3038

Wang D, Liang J, Zhang H, Zhang J (2022): Reinvestigation of Ferrate(VI) Oxidation of Bisphenol A over a Wide pH Range. ACS ES&T Water 2, 156-164

Wang N, Wang NN, Tan L, Zhang R, Zhao Q, Wang HB (2020): Removal of aqueous As(III) Sb(III) by potassium ferrate ($K_2FeO_4$): The function of oxidation and flocculation. SCI TOTAL ENVIRON 726

Wang Z, Qiu W, Pang S, Guo Q, Guan C, Jiang J (2022): Aqueous Iron(IV)–Oxo Complex: An Emerging Powerful Reactive Oxidant Formed by Iron(II)-Based Advanced Oxidation Processes for Oxidative Water Treatment. ENVIRON SCI TECHNOL 56, 1492-1509

Xu L, Fu FL, Yu PJ, Sun GZ (2022): Properties and mechanism of Cr(VI) adsorption and reduction by $K_2FeO_4$in presence of Mn(II). ENVIRON TECHNOL 43, 918-926

Yan W, Vasic R, Frenkel AI, Koel BE (2012): Intraparticle Reduction of Arsenite (As(III)) by Nanoscale Zerovalent Iron (nZVI) Investigated with In Situ X-ray Absorption Spectroscopy. ENVIRON SCI TECHNOL 46, 7018-7026

Yang T, Liu YL, Wang L, Jiang J, Huang ZS, Pang SY, Cheng HJ, Gao DW, Ma J (2018): Highly effective oxidation of roxarsone by ferrate and simultaneous arsenic removal with in situ formed ferric nanoparticles. WATER RES 147, 321-330

Yang T, Wang L, Liu YL, Jiang J, Huang ZS, Pang SY, Cheng HJ, Gao DW, Ma J (2018): Removal of Organoarsenic with Ferrate and Ferrate Resultant Nanoparticles: Oxidation and Adsorption. ENVIRON SCI TECHNOL 52, 13325-13335

Yunho, Lee, Gerd-Joachim, Ik-Hwan, Um, Jjeyong, Yoon (2003): Arsenic(III) Oxidation by Iron(VI) (Ferrate) and Subsequent Removal of Arsenic(V) by Iron(III) Coagulation. ENVIRON SCI TECHNOL 37, 5750-5756

Zhang Y, Yang M, Dou X, He H, Wang D (2005): Arsenate adsorption on an Fe-Ce bimetal oxide adsorbent: role of surface properties. ENVIRON SCI TECHNOL 39, 7246–7253

Zheng Q, Tu S, Hou J, Ni C, Wang M, Ren L, Wang M, Cao M, Xiong S, Tan W (2021): Insights into the underlying mechanisms of stability working for As(III) removal by Fe-Mn binary oxide as a highly efficient adsorbent. WATER RES 203, 117558

# Figures

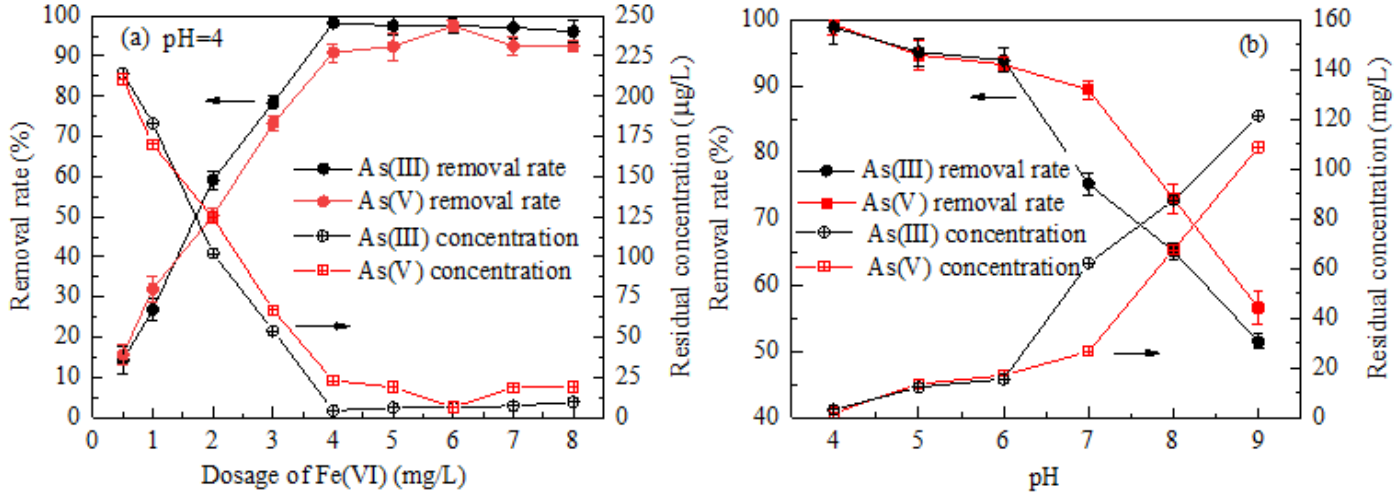


**Figure 1**

Effect of Fe(VI) dosage and pH on As(V) and As(III) removal (initial concentration of arsenic 250 μg/L). (a) influence of Fe(VI) dosage (b) the influence of pH on As(V) removal at Fe(VI) dosage 6 mg/L and As(III) removal at Fe(VI) dosage 4 mg/L.

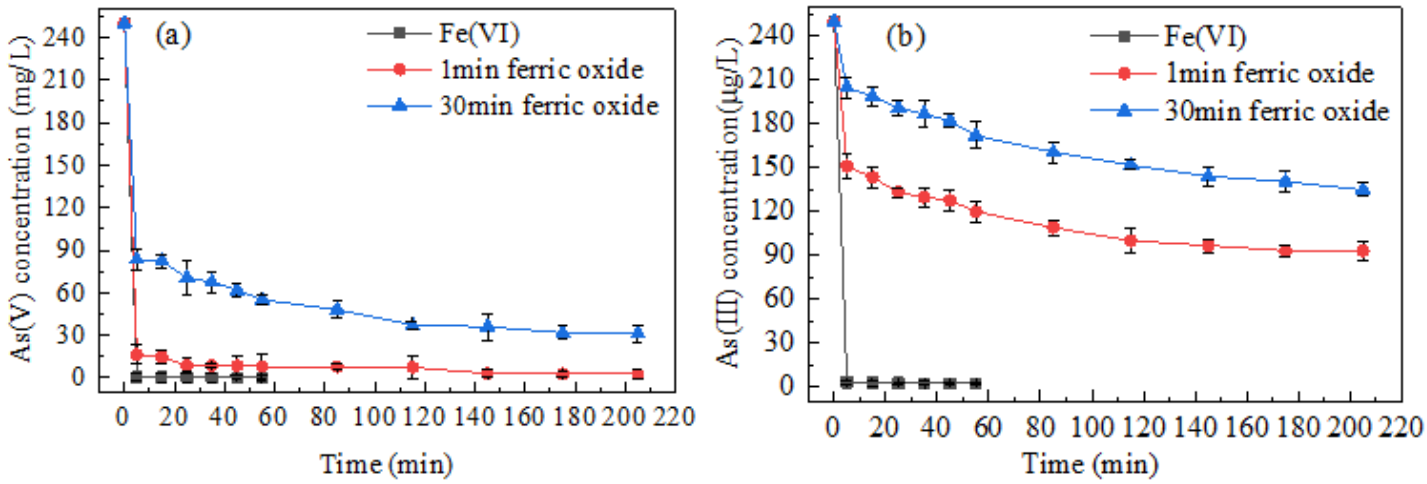


**Figure 2**

Effect of As(Ⅴ) and As(III) removal by Fe(VI) and ferric oxide at different reaction times ((a) initial As(V) concentration was 250 μg/L, Fe(VI) dosage was 6 mg/L, pH = 4.0, T = 25 °C, (b) initial As(III) concentration was 250 μg/L, Fe(VI) dosage was 4 mg/L, pH = 4.0, T = 25 °C).

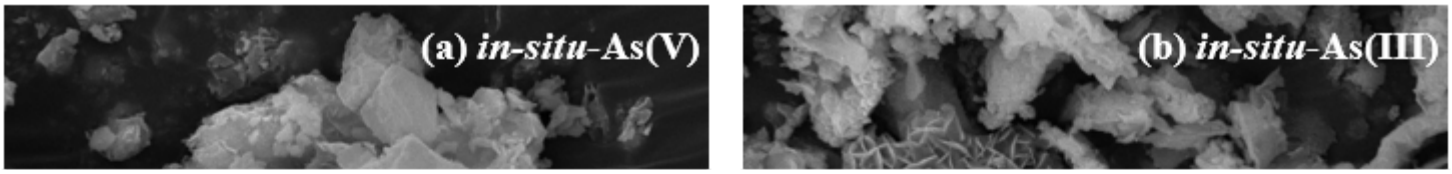


## Figure 3

SEM images of the particles formed in Fe(VI) and hydrolytic ferric iron oxides for arsenic removal (ferrate oxidation with arsenic particles (in-situ), mixture of 30 min hydrolytic ferric iron oxides particles with arsenic (ex-situ)).

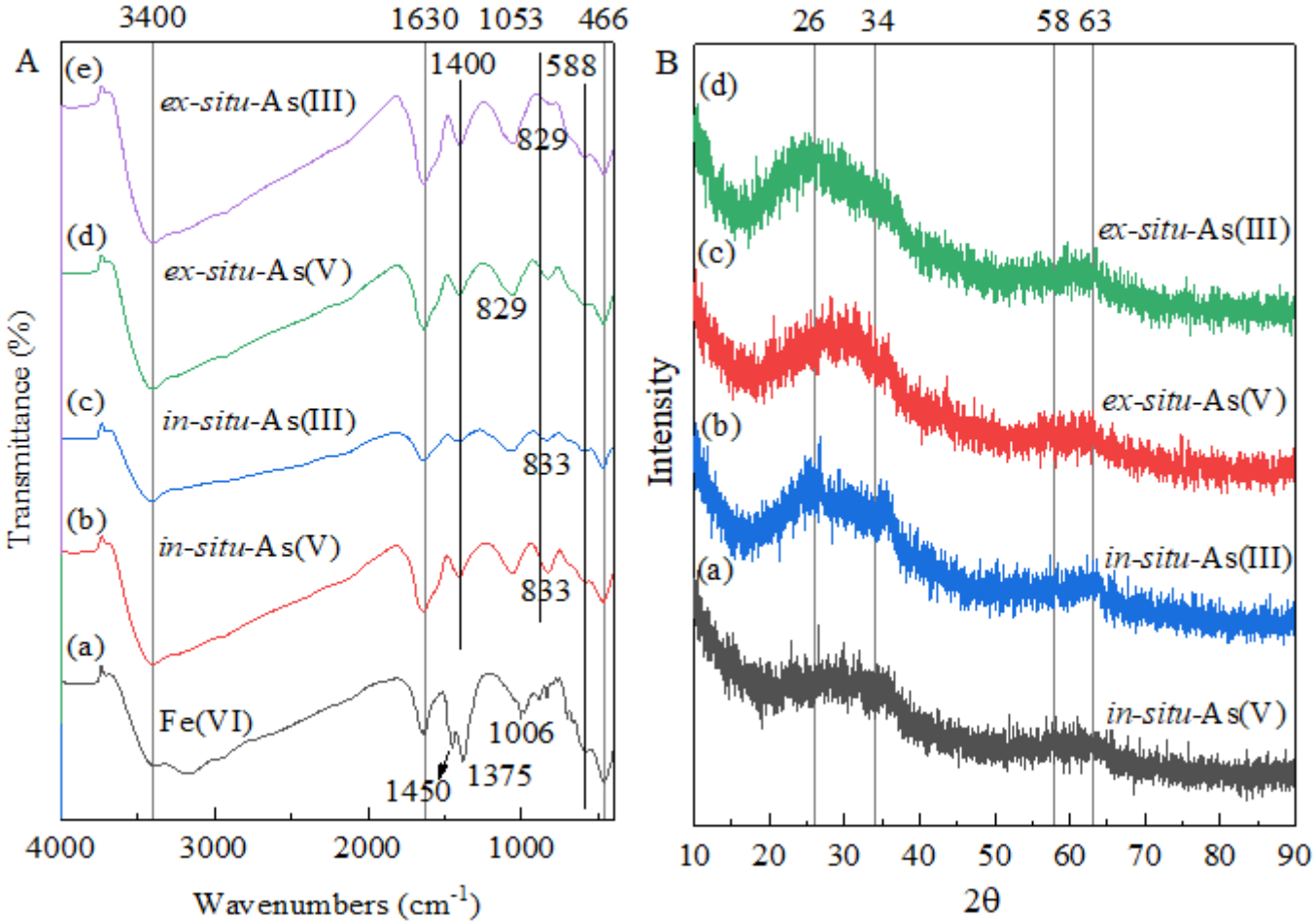


## Figure 4

FTIR spectra (A) and XRD patterns (B) of the particles formed in Fe(VI) and hydrolytic ferric iron oxides for arsenic removal (ferrate resultant particles self-decomposition (Fe(VI)), ferrate oxidation with arsenic particles (in-situ), mixture of 30 min hydrolytic ferric iron oxides particles with arsenic (ex-situ)).

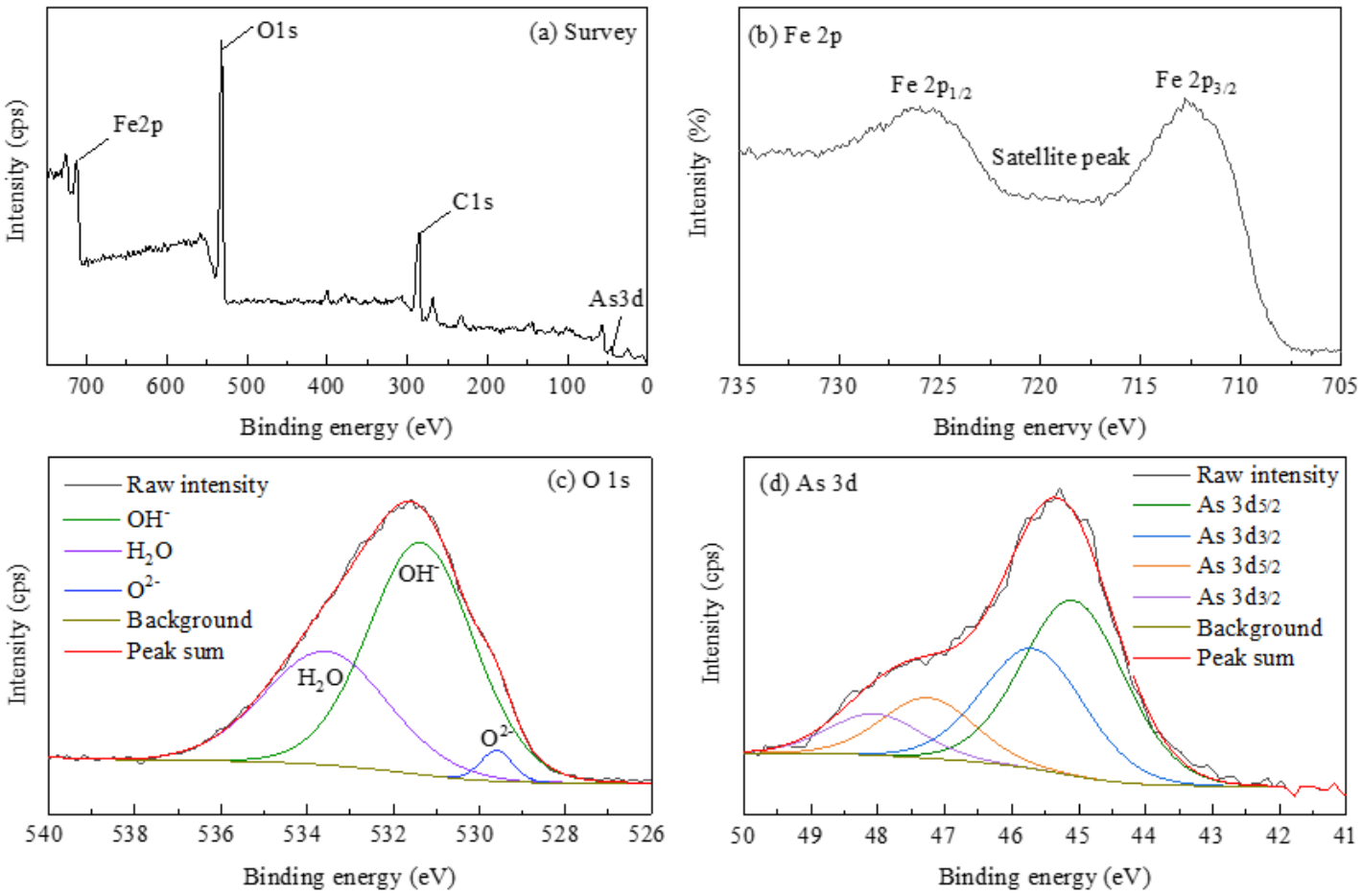


## Figure 5

XPS results of the precipitates from Fe(VI) removing As(Ⅲ) ((a) full spectrum, (b) Fe.2p, (c) O 1s (d) As 3d).

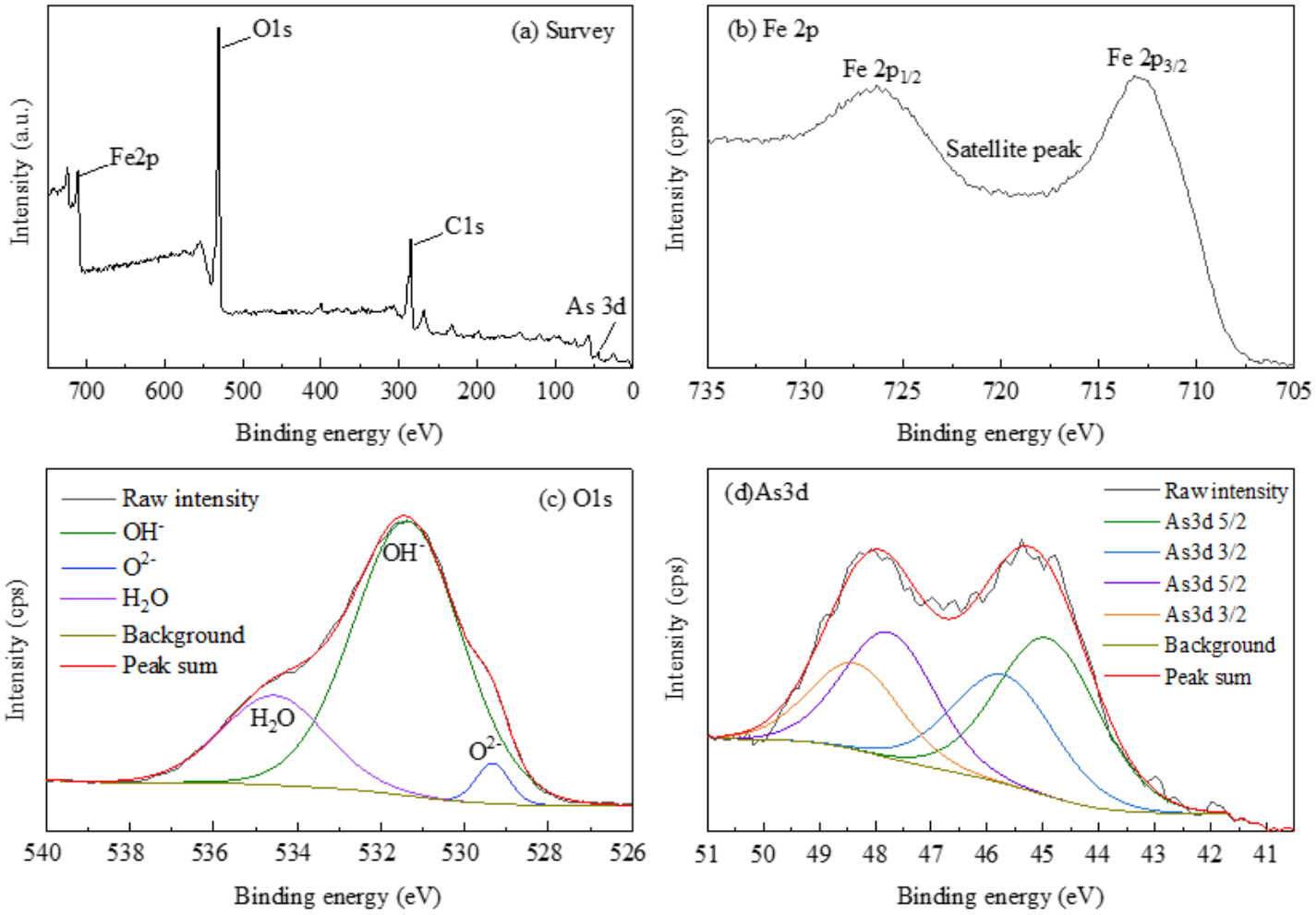


## Figure 6

XPS results of the precipitates from Fe(VI) removing As(V) ((a) full spectrum, (b) Fe.2p, (c) O 1s (d) As 3d).

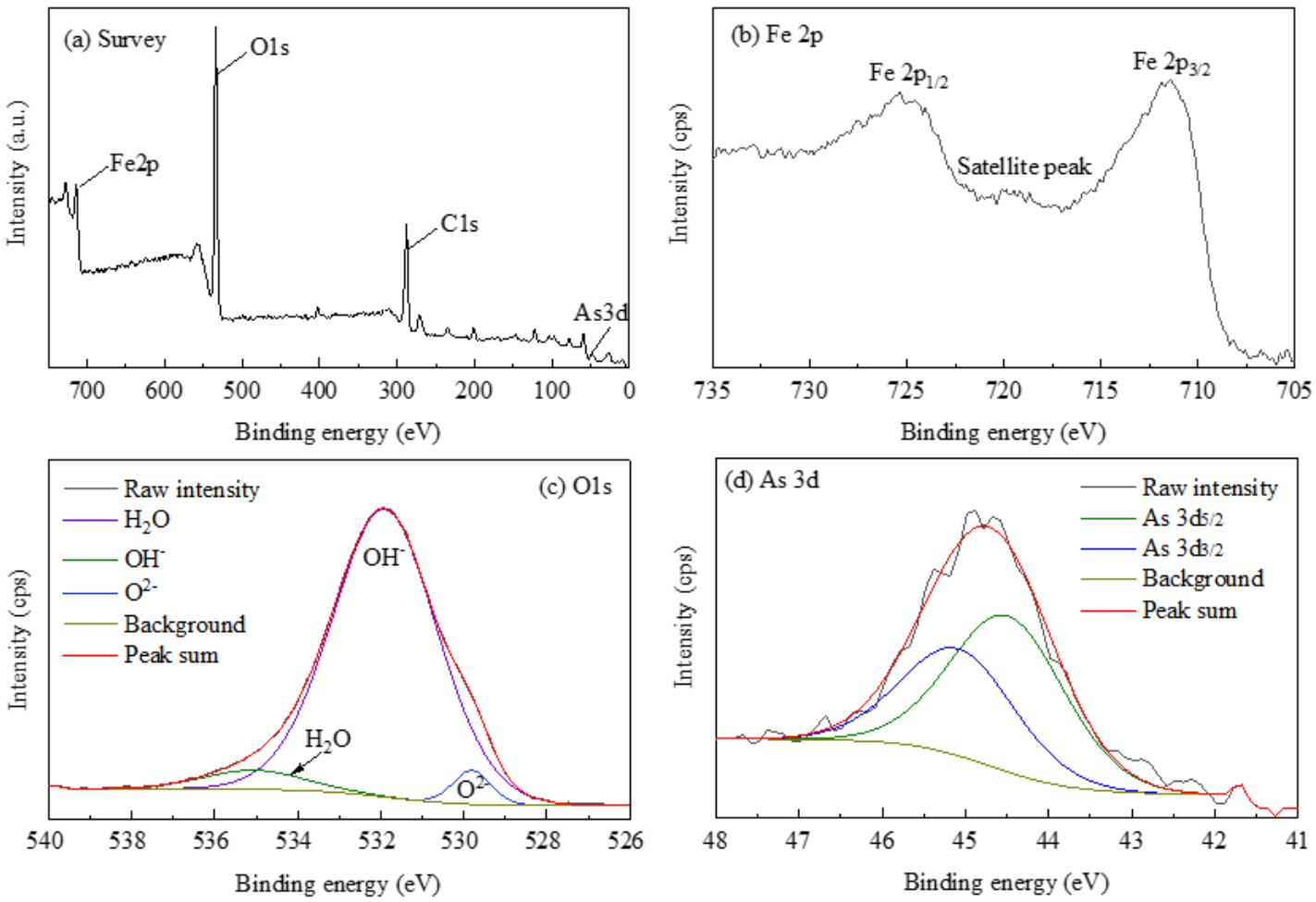


## Figure 7

XPS results of the precipitates from the 30 min hydrolytic ferric iron oxides removing As(III) ((a) full spectrum, (b) Fe.2p, (c) O 1s (d) As 3d).

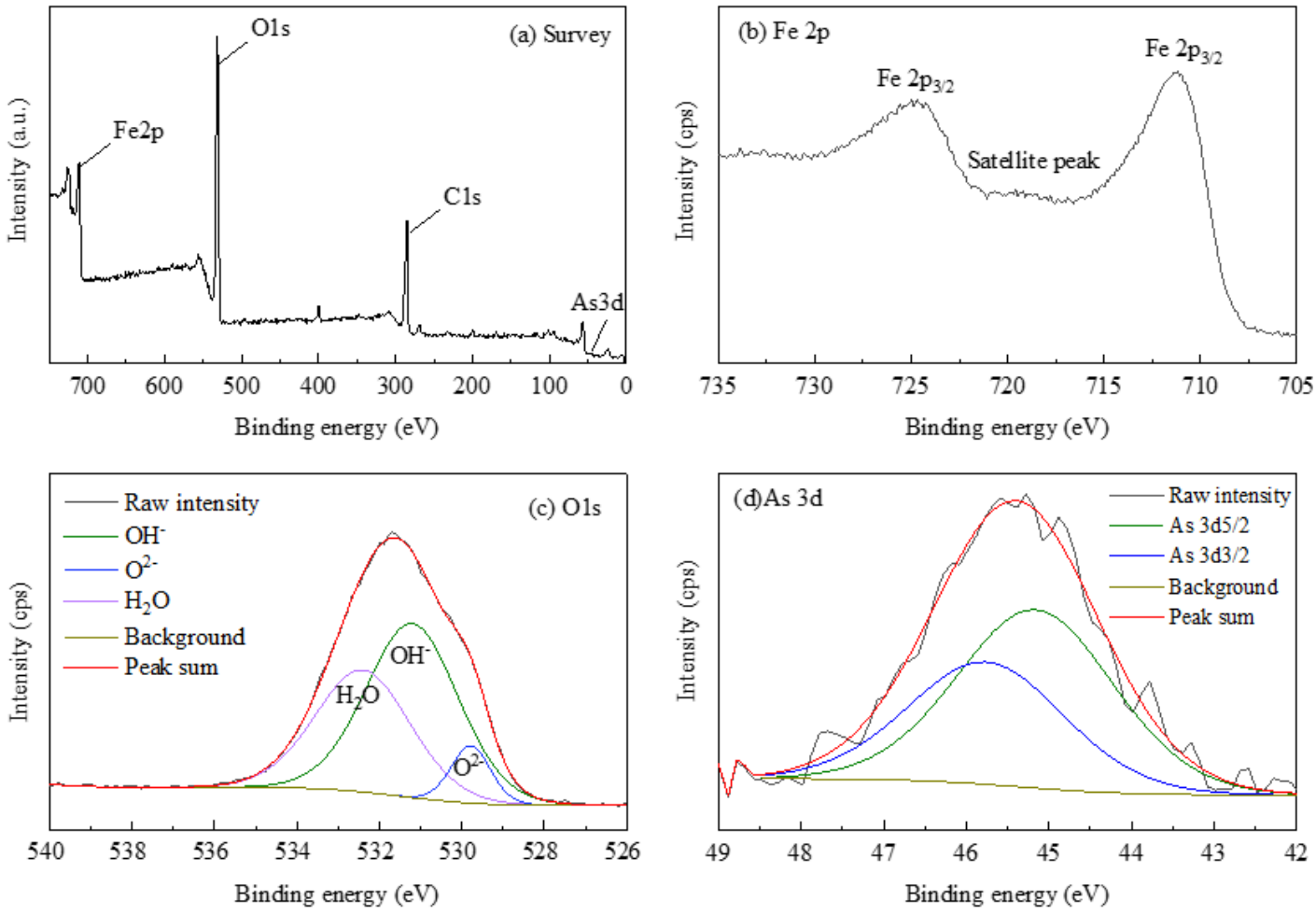


## Figure 8

XPS results of the precipitates from the 30 min hydrolytic ferric iron oxides removing As(V) ((a) full spectrum, (b) Fe.2p, (c) O 1s (d) As 3d).

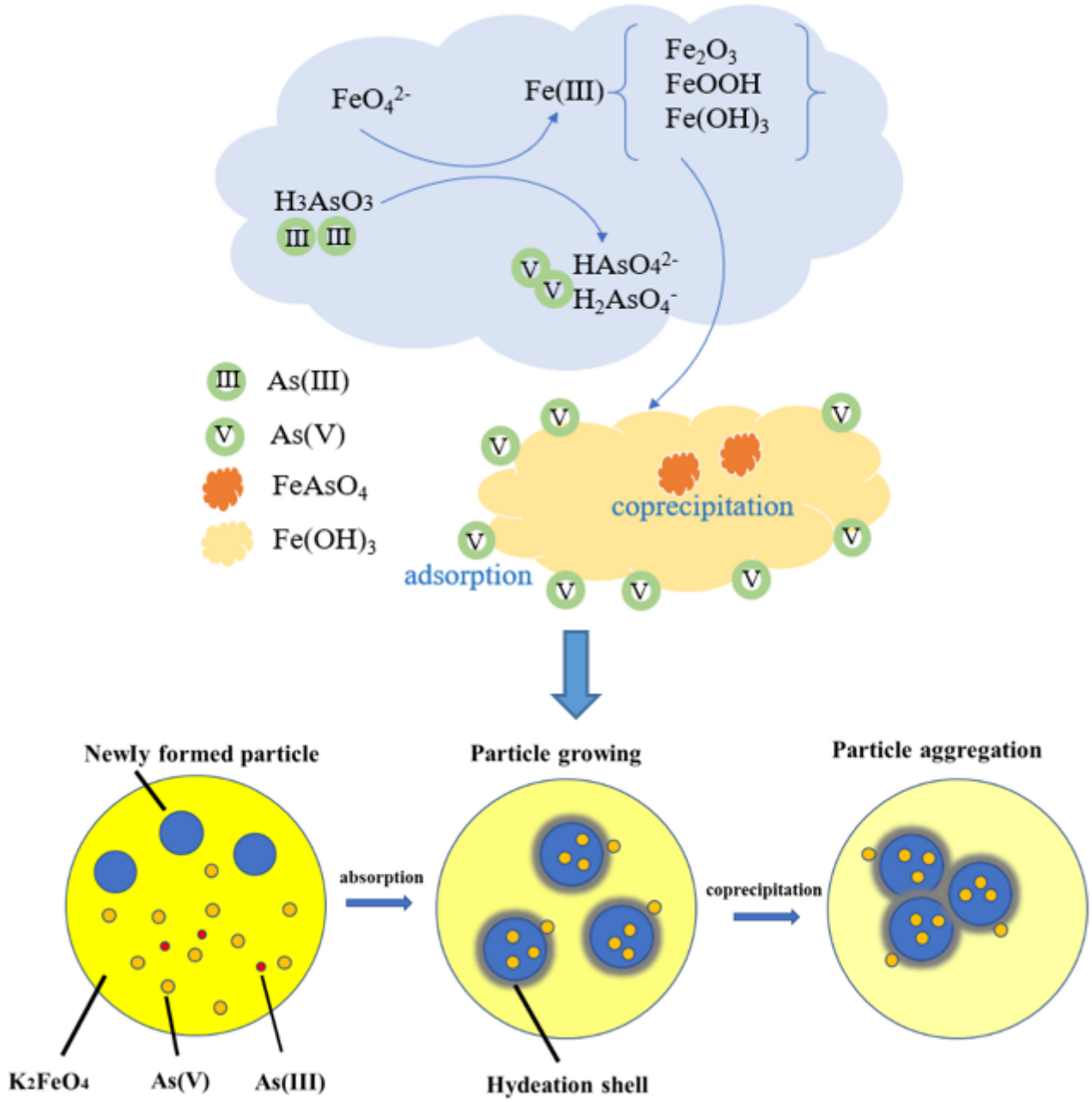


**Figure 9**

Proposed schematic diagram on arsenic by Fe(VI).

## Supplementary Files

This is a list of supplementary files associated with this preprint. Click to download.

- Supportinginformation.docx